Russell, C., Forfar, L. C., Green, M., McGrady, J. E., & Zeng, D. (2016). Probing the Structure, Dynamics, and Bonding of Coinage Metal Complexes of White Phosphorus. Chemistry - A European Journal, 22(15), 5397-5403. DOI: 10.1002/chem.201505031

FULL PAPER

Probing the Structure, Dynamics and Bonding of Coinage Metal Complexes of White Phosphorus

Laura C. Forfar,[a] Dihao Zeng,[b] Michael Green,[a] John E. McGrady*[b] and Christopher A. Russell*[a]

Abstract: A series of cationic white phosphorus complexes of the coinage metals Au and Cu have been synthesised and characterised both in the solid state and in solution. All complexes feature a P_4 unit coordinated through an edge P-P vector (i.e. η^2-like), although the degree of activation (as measured by the coordinated P–P bond length) is greater in the gold species. All the cations are fluxional on the NMR timescale at room temperature, but in the case of the gold systems fluxionality is frozen out at –90 °C. Electronic structure calculations suggest that this fluxionality proceeds *via* an η^1-coordinated M–P_4 intermediate.

Introduction

White phosphorus, P_4, represents the major industrial P-atom source for the production of organophosphorus compounds which are employed on a large scale in a wide range of technologies. The syntheses of these organophosphorus compounds involve a multistep process in which P_4 is first chlorinated or oxychlorinated to generate tri- and pentavalent phosphorus halides/oxohalides, which are subsequently functionalised by, for example, salt elimination reactions. Clearly this process is both hazardous and environmentally unfriendly. An alternative approach involving the controlled activation of P_4 leading to phosphorus-containing products without the need for direct halogenation is clearly desirable, but at the present time remains a target rather than a reality – the attainment of this goal will be underpinned by a deep understanding of the coordination chemistry of P_4.[1] Thus, despite the fact that P_4 is recognised as being a poor donor ligand, the coordination chemistry of white phosphorus in a wide variety of transition metal complexes has been studied.[2] Commonly, reactions of P_4 with transition metal fragments lead to decomposition of the tetrahedral P_4 molecule; however, coordination of the intact P_4 moiety has been observed in a number of cases, with binding either *via* an edge (*i.e.*, η^2) or a corner (*i.e.*, η^1), depending on the precise steric and electronic environment at the metal centre. In the electronically preferred η^2-mode, the resemblance between M–P_4 binding and M–alkene binding has been noted.[3]

Our own interest in this topic is part of our studies into the binding of small molecules at coinage metal centres. Thus we recently reported[4] that reactions of equimolar quantities of simple metal salts MX (M = Au, Cu, X = Cl; M = Ag, X = OTf) and $GaCl_3$ in CH_2Cl_2 with P_4 led to phosphorus ligating a cationic coinage metal centre. For Cu and Ag, ion-contacted coordination polymers are formed; for Au, an ion-separated complex is observed that features the $[Au(\eta^2\text{-}P_4)_2]^+$ cation. The observation of these different structures was rationalised using a simple thermodynamic cycle complemented by gas-phase quantum chemical studies which showed weak M–P_4 interactions. The formation of $[M(\eta^2\text{-}P_4)_2]^+$ is rather endothermic for M = Cu, Ag, allowing competitive formation of coordination polymers *via* M–Cl links. The nature of the M–P_4 bond in complexes of this type has been the matter of some discussion, dating back to Ginsberg and Welch's earliest discussions of the electronic structure of $RhCl(\eta^2\text{-}P_4)(PPh_3)_2$ using extended Hückel and SCF-X_α theory.[3, 5] The coordinated P–P bond in this case is significantly elongated from its equilibrium value in P_4 (2.4616(22) Å vs 2.1994(3) Å from gas-phase electron diffraction[6]). The synergic nature of the bonding (and hence the analogy to the familiar Dewar-Chatt-Duncanson binding model[7] for ethene) was noted at this point: donation of electron density from the P–P σ bond to the metal and back-donation of metal d electrons into P–P σ^* may both contribute to the overall stability of the complex. Following the report of the $[Ag(P_4)_2]^+$ cation,[8] Krossing and van Wüllen argued that the coordinated P–P bond length of 2.329(2) Å was in fact a truer signature of an η^2-P_4 coordination mode, and that the rhodium complex was better formulated as a κ^2-$[P_4]^{2-}$ complex of Rh(III).[2a] Subsequent calculations by Deubel confirmed the importance of back-bonding, even in the complex of Ag^+, but also suggested that the planar (D_{2h}) cordination geometry about Ag^+ was the result of inter- rather than intramolecular factors.[8] Despite the differences of opinion that have emerged in these papers, the synergic nature of the bonding is not in doubt, and it seems clear that all P_4 complexes that are bound *via* two phosphorus atoms lie comewhere on a continuum whose limits are M(I)(η^2-P_4) and M(III)(κ^2-P_4).

[a] *Dr Laura C. Forfar, Prof.. Michael Green, Dr. Christopher A. Russell*
School of Chemistry
University of Bristol
Cantock's Close, Bristol, BS8 1TS, United Kingdom
E-mail: chris.russell@bristol.ac.uk
[b] *Dihao Zeng, Prof. John E. McGrady*
Department of Chemistry
University of Oxford
South Parks Road, OX1 3QZ, United Kingdom
E-mail: john.mcgrady@chem.ox.ac.uk

Supporting information for this article is available on the WWW under http://dx.doi.org/

The rich coordination chemistry that has emerged in these apparently simple systems prompted us to seek a greater understanding of these M–P_4 interactions by introducing co-ligands at the metal centres. Herein we present a combined synthetic, solid-state, solution and computational analysis of these complexes.

Results and Discussion

Synthesis and structure

Our synthetic approaches towards these complexes are shown in Scheme 1 and involves the initial reaction of CH_2Cl_2 solutions of [LMX] with $GaCl_3$ or $AgSbF_6$ {L = P(^{t}Bu)$_2$(*o*-biphenyl) (JohnPhos), P(^{t}Bu)$_2$(2',4',6' -triisopropylbiphenyl) (^{t}BuXPhos) or 1,3-bis(2,6-diisopropylphenyl)-1,3-dihydro-2H-imidaz-ol-2-ylidene(IPr)} followed by the addition of one equivalent of white phosphorus.

The resulting solutions are, in the cases of the gold complexes **1**–**3** (Scheme 1), clear and colourless, which display broad $^{31}P\{^1H\}$ resonances (CD_2Cl_2, RT) for the P_4 moiety that are significantly downfield from that of free P_4 under the same conditions (**1**, δ ≈ –454 ppm; **2**, δ ≈ –455 ppm; **3**, δ ≈ –465 ppm; *cf.* free P_4 at δ ≈ –525 ppm). It is interesting to note that, for complex **1**, reactions with sub-stoichiometric equivalents of P_4 gave solutions which showed additional peaks in the $^{31}P\{^1H\}$ NMR spectrum which, although they cannot be definitively assigned, are suggestive of more complex coordination chemistry. Furthermore. reactions of Type A were attempted using Cu compounds; again $^{31}P\{^1H\}$ NMR was indicative of complexation of the P_4 unit but the samples coudl not be purified and no further chracteristaion was attempted.

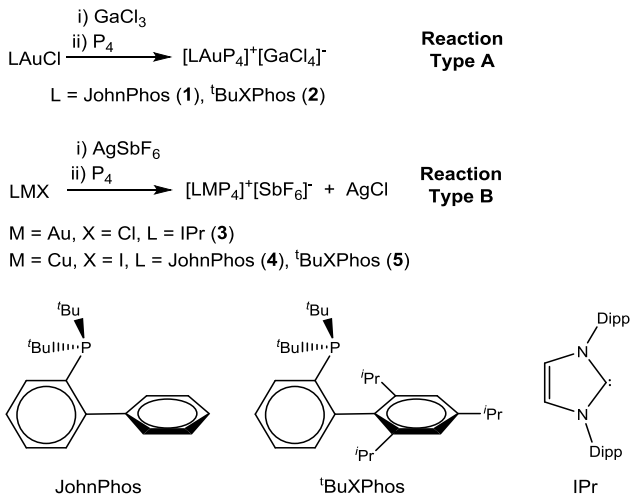

Scheme 1. Reactions used to prepare **1**–**5**.

In contrast, the copper complexes **4** and **5** form intensely yellow coloured solutions that display $^{31}P\{^1H\}$ NMR signals (CD_2Cl_2, RT) for the P_4 moiety at δ ≈ –468 ppm (**4**) and δ ≈ –493 ppm (**5**) respectively. It is noteworthy that in all cases **1**–**5**, the room temperature NMR spectra gave chemical shifts characteristic of an intact P_4 cage, and that in each case only a solitary signal for the P_4 moiety was observed, suggesting that a dynamic process is occurring on the NMR timescale leading to the single time-averaged signal.

Crystals of **1**–**5** were grown that were suitable for analysis by single crystal X-ray diffraction experiments (molecular structures of the cations are shown in Figure 1; key bond dimensions are given in Table 1). The solid state structure of [{P^{t}Bu$_2$(*o*-biphenyl)}Au(η^2-P_4)][$GaCl_4$] (**1**) shows P_4 binding symmetrically to gold in an η^2-fashion with a coordinated P–P bond length of 2.341(3) Å, somewhat longer than that in free P_4 (2.20 Å) but shorter than that in the $[Au(P_4)_2]^+$ cation (2.410(1) Å).[9] The coordinated P–P bond lies perpendicular to the approximate mirror plane passing through Au, P(5) and the *ipso* carbon. In subsequent discussions we refer to this orientation as the *horizontal* isomer. The other P–P bonds in the P_4 unit are slightly contracted {2.155(5)–2.210(6) Å} compared to those in free P_4, a common feature in P_4 coordination chemistry. The Au(1)–P(1,2) bond distances of 2.442(2) Å and 2.446(2) Å are statistically equivalent, and P(5)–Au(1)–P(2,3) angles are 148.97(8) and 150.67(7)° respectively. The P(5)–Au(1)-PP$_{centroid}$ angle is close to linear at 169.9°, with minimal interaction with the flanking aromatic ring of the o-biphenyl group of the JohnPhos ligand (the closest contact is Au(1)–C$_{ipso}$ at 3.124(9) Å, which, according to a report by Echavarren *et al.,* is indicative of a very weak interaction between the two atoms[10]).

The coordination of the P_4 unit may be altered by employing a more sterically encumbered phosphine ligand, in this case ^{t}BuXPhos. The solid-state structure of [{^{t}BuXPhosAu}(η^2-P_4)][$GaCl_4$] (**2**) again shows the P_4 tetrahedron bonded to the gold centre in an η^2- fashion, but the coordinated P–P bond is now rotated by approximately 90° relative to **1**, such that it lies in the mirror plane (defined by Au–P(5)–C$_{ipso}$) rather than perpendicular to it (the *vertical* coordination mode). Moreover, the coordinated P–P bond is rather longer than that in P(^{t}Bu)$_2$(*o*-biphenyl) {2.4182(8) Å *vs* 2.341(3) Å)} but the Au(1)–P(5) distance is the same within error {2.3301(5) Å vs 2.3218(18) Å}. The Au–P(1) and Au-P(2) bonds are also now distinctly asymmetric: 2.4067(6) Å and 2.4869(6) Å, respectively, while the P(5)–Au(1)–P(1) and P(5)–Au(1)–P(2) angles are 171.309(2)° and 128.274(2)°, respectively. The overall coordination geometry defined by the three phosphorus donor atoms is therefore, to a first approximation, T-shaped. In the context of the M(I)(η^2-P_4) and M(III)(κ^2-P_4) continuum discussed in the introduction, it appears that the binding in **2** is significantly displaced towards the M(III)(κ^2-P_4) end, as judged by the P–P distance and also the characteristic switch from approximately tetrahedral (**1**) to approximately planar (**2**) coordination geometries at the metal. We return to this point in the discussion of electronic structure.

In order to further increase the electron donating character of the ligand,[11] we also synthesised the corresponding *N*-heterocyclic carbene complex [{IPrAu}(η^2-P_4)][SbF_6] (**3**). The solid-state structure of **3** again shows white phosphorus coordinated to gold in an η^2-

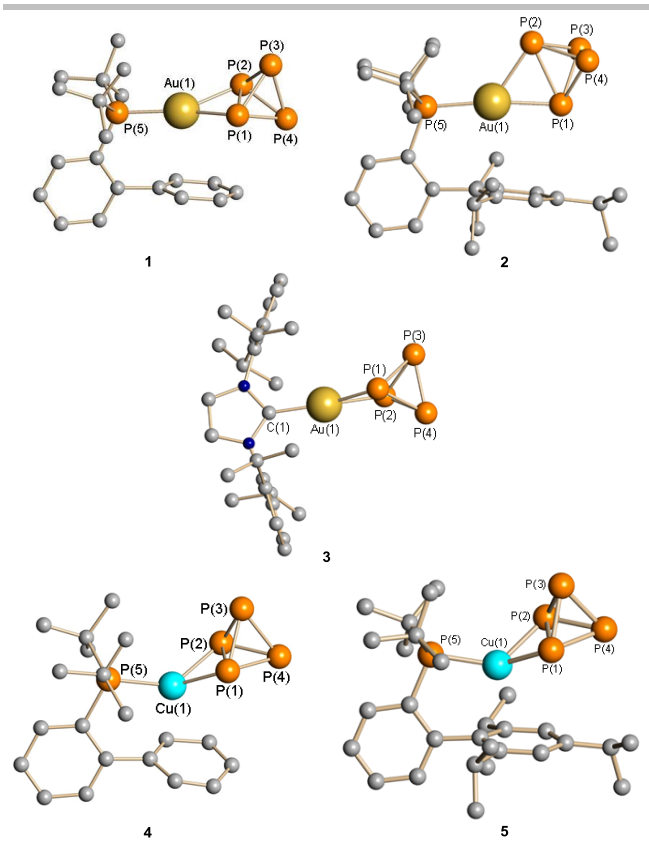

Figure 1. Molecular structures of the cations of **1**, **2**, **3**, **4** and **5**. In all cases the anions and all hydrogen atoms have been omitted for clarity.

fashion, and the horizontal coordination mode is much more similar to **1** than **2**. The Au–P(1,2) distances of 2.4333(7) Å and 2.4352(6) Å are statistically identical, the coordinated P–P bond is 2.357(1) Å {*cf.* 2.341(3) Å in **1**} and the coordination geometry again approximates trigonal planar. Thus it appears that the steric bulk ([P^{t}Bu$_2$(*o*-biphenyl) *vs* ^{t}BuXPhos) has a greater impact on the P–P distance than the donor properties of the ligand (P^{t}Bu$_2$(*o*-biphenyl) *vs* IPr).The solid-state structures of the copper analogues of **1** and **2** (**4** and **5**, respectively) showed the P_4 unit again binding to the copper(I) centre in an η^2- fashion, but in both cases the horizontal coordination mode is preferred, reminiscent of **1** and quite distinct from **2**. The coordinated P–P bonds again lengthen, but to a lesser extent than observed in **1** (2.285(3) Å (**4**) and 2.2912(12) Å (**5**) vs 2.341(3) Å in **1**). These values are also distinctly shorter than the coordinated P–P bond in the copper–P_4 coordination polymer previously reported in our group {2.3744(7) Å}. In both **4** and **5** the Cu makes close contacts with the C_{ortho}–C_{ipso} edge of the flanking arene ring {2.302(7) Å (**4**) and 2.324(2) Å (**5**)} and the P_4 moiety is tilted away from the biphenyl unit. Echavarren *et al.* noted a similar distortion in a related copper complex of acetonitrile.[10] We comment further on the significance of the interaction of the arene with the metal in the subsequent discussion of electronic structure.

Table 1. Key bond dimensions of the cations of **1**, **2, 3**, **4** and **5**.

	1	**2**	**3**	**4**	**5**
M-P(1)	2.442(2)	2.4067(6)	2.4352(6)	2.310(4)	2.3253(11)
M-P(2)	2.446(2)	2.4869(6)	2.4333(7)	2.315(4)	2.3602(12)
M-L[a]	2.3218(18)	2.3301(5)	2.035(2)	2.243(4)	2.2535(10)
P(1)-P(2)	2.341(3)	2.4182(8)	2.3571(10)	2.281(5)	2.2912(12)
P(1)-P(3)	2.171(4)	2.1981(9)	2.1666(10)	2.165(6)	2.1873(12)
P(1)-P(4)	2.155(5)	2.1799(8)	2.1642(11)	2.160(5)	2.1728(12)
P(2)-P(3)	2.174(4)	2.1697(9)	2.1704(10)	2.177(6)	2.1668(13)
P(2)-P(4)	2.167(4)	2.1686(9)	2.1704(11)	2.174(6)	2.1893(13)
P(3)-P(4)	2.210(6)	2.1967(10)	2.1941(11)	2.225(7)	2.2192(13)
L-M-PP$_{centroid}$	169.9	157.1	175.4	138.0	137.1

[a] Distance between M and the donor atom of the supporting ligand (*i.e.*, either the P of PR_3 or the C of NHC)

NMR spectroscopy

The $^{31}P\{^1H\}$ NMR spectrum of **1** gives a broad signal at $\delta_P \approx 75$ ppm for the phosphine ligand and a broad peak at –454 ppm for the P_4 ligand, consistent with a dynamic process leading to scrambling of all four phosphorus atoms of the P_4 cage. This may originate from an intramolecular process involving the "tumbling" of the P_4 tetrahedron that interconverts the coordinated and non-coordinated phosphorus centres, or alternatively a process involving breaking the M–P_4 bond and subsequent rebinding. We note that a dynamic process exchanging, in both solution and solid state, the P-atoms of mononuclear and dinuclear white phosphorus complexes has been reported.[12] Previously isolated $[M(P_4)_2]^+$ (M = Cu,[13] Ag,[14] Au[9]) compounds also exhibit rapid fluxionality which could not be frozen out even at temperatures as low as –90 °C. In contrast, variable

temperature ^{31}P NMR spectroscopy on **1** proved to be more revealing (Figure 2). Cooling **1** to –20 °C causes the resonance at 75 ppm {P(5)} to resolve into an apparent quintet, due to coupling to four phosphorus atoms of the P_4 unit {P(1–4)} that appear equivalent on the NMR timescale. The quintet for this resonance is also observed at –40 and –60 °C, but at –80 and –90 °C the multiplicity of this peak changes to a triplet. The anticipated triplet of triplets was not observed, presumably because the 3-bond coupling to the non-coordinated phosphorus atoms is not resolved. The resonance due to the P_4 unit is similarly temperature dependent: at –60 °C the broad peak at $\delta_P \approx$ –454 ppm resolves into a broad doublet which becomes complex multiplet at –90 °C, resulting from the two different phosphorus environments in the P_4 unit coupling to each other and to P(5). The second order splitting pattern has been modelled as an A_2MX_2 spin system (see Supporting Information).

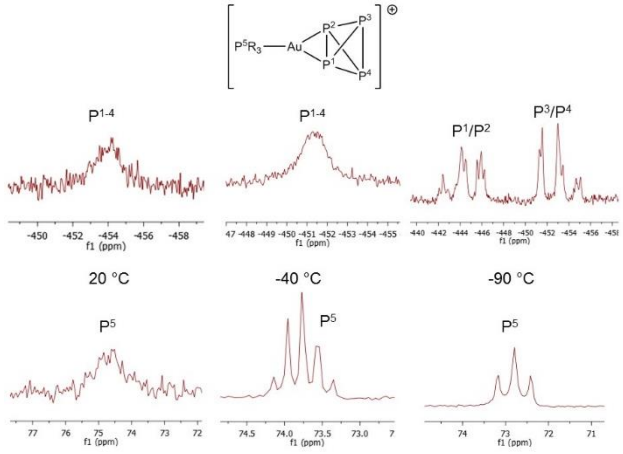

Figure 2. Variable temperature $^{31}P\{^1H\}$ NMR spectra of CD_2Cl_2 solutions of **1**.

The $^{31}P\{^1H\}$ NMR spectra of **2** shows the same general pattern as **1**, with two singlets at $\delta_P \approx$ 73.2 {P(5)} and –454.8 {P(1–4)} ppm at room temperature. Cooling to –40 °C leads to broadening of the peak at –454 ppm and splitting of the 73 ppm resonance into a quintet. At –90 °C, the peak at $\delta_P \approx$ 73 ppm resolves into a triplet and the peak for the P_4 tetrahedron generates the same second order splitting pattern as described above for **1**. The room temperature spectrum of **3** also gives a very broad signal at $\delta_P \approx$ –465 ppm, which resolves into a triplet at –460.4 and a broad peak at –450 ppm upon cooling to –90 °C. The room temperature $^{31}P\{^1H\}$ NMR spectra of the copper analogues, **4** and **5**, also show sharp singlets for the P_4 unit at $\delta_P \approx$ –467.7 ppm (**4**) and –492.9 ppm (**5**) and a broad singlet for the phosphine ligand at $\delta_P \approx$ 29.3 ppm (**4**) and 28.6 ppm (**5**). Even at –90 °C, however, the resonances for the P_4 unit do not resolve into a second order splitting pattern.

Computational analysis

In an attempt to rationalise the observed structural and spectroscopic trends, we have used density functional theory to explore the potential energy surfaces for **1**, **2**, **4** and **5**. The optimised structure of **1** shown in Figure 3 (**1-h**) is very similar to the X-ray data, with the P_4 unit adopting a horizontal coordination mode. The coordinated P–P bond is somewhat longer than in the experiment {2.41 Å vs 2.341(3) Å} but the Au-C_{ipso} distance of 3.10 Å matches well with the crystallographic value of 3.124(9) Å. The coordinated P–P bonds are systematically over-estimated by ~0.06 Å in all systems studied here, and the same trend has also emerged in other studies (see for example Table 1 in reference 7). We have also located a second local minimum for **1** (**1-v**, corresponding to the vertical coordination mode seen in **2**) only very marginally less stable than the global minimum (+8 kJ/mol). The coordination geometry is approximately square planar, with a longer coordinated P–P bond (2.45 Å in **1-v** *vs* 2.41 Å in **1-h**), two quite distinct Au–P distances of 2.45 Å (*trans* to PR_3) and 2.52 Å (*trans* to the aryl group). The fourth coordination site is filled by a C=C double bond from the arene ring which is brought into bonding distance of the metal by a distinct tilt, leading to very asymmetric Au–C_{ortho} distances of 3.20 Å and 3.61 Å. The tilting of the arene ring in **1-h** is much less pronounced, (Au–C_{ortho} = 3.33 Å and 3.42 Å), suggesting a weaker interaction. It is interesting to note that the Au-C_{ipso} distances are rather similar in **1-h** and **1-v** (3.10 Å and 3.13 Å, respectively), and so the asymmetry in Au-C_{ortho} distances, rather than the Au-C_{ipso} distance in isolation, appears to be the best gauge of the strength of the metal arene interaction in these cases. Analysis of the topology of the electron density reveals a bond critical point at the midpoint of the coordinated P-P bond in both **1-h** and **1-v**, although the density is somewhat smaller in the latter (0.068 e Å^{-3} in **1-v** vs 0.073 e Å^{-3} in **1-h** and 0.078 e Å^{-3} in $[Ag(P_4)_2]^{+}$[2a]). The structural information and the computed densities therefore converge to suggest that two minima, **1-h** and **1-v**, map part of the continuum between Au(I)(η^2-P_4) and Au(III)(κ^2-P_4) limits, the square planar geometry being highly characteristic of the latter.

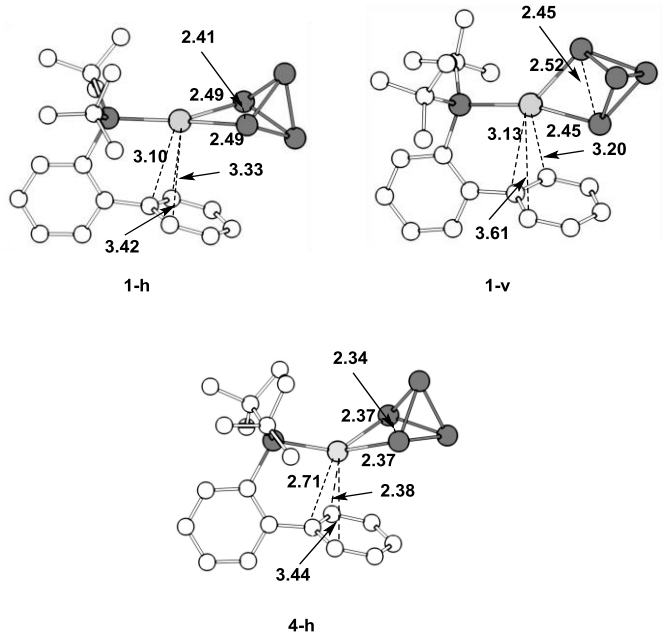

Figure 3. DFT-optimised structural parameters for **1-h**, **1-v** and **4-h.**

In the case of **2**, we have been able to identify only a single minimum corresponding to vertical isomer (**2-v**): all attempts to locate the alternative horizontal form resulted in rotation of the P_4 unit. Steric effects therefore clearly play a critical role in pushing the P_4 unit into the vertical coordination position, where donation from the arene ring can be used to maximum effect. In the copper analogues, **4** and **5**, we have also located only a single local minimum corresponding to an η^2-coordination mode, in this case the horizontal rather than vertical isomer. As was the case for the gold complexes, the coordinated P–P bond length is overestimated by ~0.06 Å, but the geometry is otherwise in excellent agreement with experiment. The structures differ from **1-h** in that the arene ring is now distinctly tilted such that one C=C double bond occupies the fourth coordination site, but in this case of an approximately tetrahedral Cu centre. These subtle differences in structure between gold and copper complexes are entirely consistent with well-established trends: the tendency of **1-h** to remain 3-coordinate and planar while **4-h** is 4-coordinate and tetrahedral is typical of the coordination chemistry of the late transition members of the first and third transition series (contrast, for example, $Pt(CO)_3$ *vs* $Ni(CO)_4$).

As noted above, the fluxionality of the P_4 unit is, in principle, consistent with a number of reaction pathways. The potential energy surface for **1** is shown in Figure 4, including the horizontal and vertical isomers discussed above. **1-h** and **1-v** are connected *via* a low-lying transition state (**1-TS0** in Figure 4, +12 kJ/mol), very similar to Krossing and van Wüllen's value of 5 kJ/mol for the difference between D_{2h}- and D_{2d}-symmetric structures of $[Ag(P_4)_2]^+$, from which we conclude that effectively free rotation of the P_4 cluster about the Au–PR_3 axis (*i.e.* along the bisector of the coordinated P-P bond) occurs in solution at all temperatures. We have also identified a low-lying η^1-coordinated intermediate, **1-I**, approximately 29 kJ/mol above the global minimum. The P–Au–P angle is now almost perfectly linear and P–P bonds lie in the range 2.19–2.25 Å, all of which is very characteristic of an Au(I) oxidation state and a largely unactivated P_4 unit. In reference 2a, isomers of $[Ag(P_4)_2]^+$ with η^1-P_4 coordination modes were located in a similar energy range (+27 kJ/mol) but were identified as saddle points rather than minima. The transition state, **1-TS1** is structurally very similar to **1-I** and lies marginally higher at +41 kJ/mol. We note, however, that the precise height of the η^1-η^2 barrier is rather dependent on methodology – at the B3LYP-D3 level it is only 27 kJ/mol while with MP2 it rises to +63 kJ/mol, more consistent with the observation that the bound and unbound phosphorus atoms can be distinguished at –90 °C.

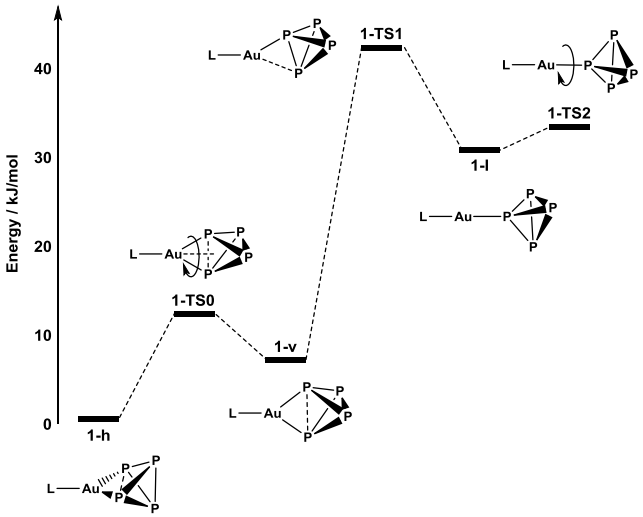

Figure 4. Potential energy surface for the dynamic processes in **1** (BP86-D3).

Conclusions

A series of novel $[LM(I)–P_4]^+$ (M = Au, Cu) complexes have been synthesised and structurally characterised. Their solid-state structures highlight the effect of the auxiliary ligand on the coordination mode of white phosphorus. In the case of gold, the coordination chemistry is typical of heavier transition elements: there is a distinct preference for planar coordination over tetrahedral, and also a marked shift towards Au(III) *vs* Au(I) character. The Au(III) character is revealed by the adoption of square planar geometries (with the arene ring filling the fourth coordination site) and the elongation of the coordinated P–P bond. In contrast, the coordination chemistry of the copper analogues is very typical of Cu(I), featuring approximately tetrahedral geometries with a C=C bond of the arene again filling the fourth coordination position. All the complexes were fluxional in solution and, in the case of the gold, the dynamic process

can be frozen out at –90 °C to reveal distinct resonances. Calculations indicate that the fluxionality occurs *via* an η^1-coordinated M(I) intermediate where the P_4 unit is deactivated.

Experimental Section

General Experimental

All reactions were performed under an atmosphere of nitrogen using standard Schlenk or glove box techniques; solvents were dried using an Anhydrous Engineering Grubbs-type system (alumina columns). White phosphorus was obtained as a generous gift from Rhodia plc and purified according to a procedure described previously.[4] The gold complexes [P^{t}Bu$_2$(*o*-biphenyl)AuCl] and [P(^{t}Bu)$_2$(2',4',6'-triisopropylbiphenyl)AuCl] were prepared according to modified literature methods[15] from tetrachloroauric(III) acid donated by Umicore. [(IPr)AuCl] (IPr = 1,3-bis[2,6-diisopropylphenyl-imidazol-2-ylidene]) was used as received from the supplier. [P^{t}Bu$_2$(*o*-biphenyl)CuI] and [P(^{t}Bu)$_2$(2',4',6'-triisopropylbiphenyl)CuI] were prepared by addition of the desired phosphine to a methanol solution of copper(I) iodide and refluxing overnight to yield a white precipitate. All other reagents were of analytical grade and obtained from commercial suppliers and were used without further purification.

^{31}P NMR spectra were obtained using a Jeol ECS 400 MHz multinuclear spectrometer. ^{1}H and ^{13}C spectra were referenced to internal solvent peaks, ^{31}P NMR spectra were referenced to an external sample of 85% H_3PO_4

Complexes **1**-**5** were prepared by either Reaction Type A (**1** and **2**) or Reaction Type B (**3**-**5**) as shown in Scheme 1. General synthetic procedures for each reaction type are given followed by specific characterisation data for each complex.

Reaction Type A: White phosphorus (0.05 mmol, 6 mg) was added to a solution containing 0.05 mmol of LAuCl {L = JohnPhos or tBuXPhos) and $GaCl_3$ (0.05 mmol, 9 mg) in dichloromethane (3 mL). The solution was stirred for 1 h in the absence of light then filtered through Celite and washed with dichloromethane (2 × 2 mL). The resulting solutions were concentrated and crystals were grown from CH_2Cl_2/hexane layers. Yields were quantitative by ^{31}P NMR spectroscopy.

Data for 1: Crystalline yield: 15 mg (36%). **^{1}H NMR** (400 MHz, 20 °C, CD_2Cl_2) δ_H 7.88 (m, Ar*H*, 1H), 7.62 (m, Ar*H*, 1H), 7.53 (t, Ar*H*, 1H), 7.45 (t, Ar*H*, 1H), 7.28-7.20 (m, Ar*H*, 2H), 1.45 (d, $J_{H\text{-}P}$ = 16.3 Hz, C(CH_3)$_3$, 18H) ppm; **^{13}C NMR** (100 MHz, 20 °C, CD_2Cl_2) δ_C 148.88 (d, $J_{C\text{-}P}$ = 13.7 Hz), 143.77 (d, $J_{C\text{-}P}$ = 6.5 Hz), 135.16 (s), 133.96 (d, $J_{C\text{-}P}$ = 7.8 Hz), 132.29 (d, $J_{C\text{-}P}$ = 2.5 Hz), 130.54 (s), 130.40 (s), 130.03 (s), 128.70 (d, $J_{C\text{-}P}$ = 7.4 Hz), 125.85 (d, $J_{C\text{-}P}$ = 44.9 Hz), 39.20 (d, $^1J_{C\text{-}P}$ = 21.3 Hz), 31.26 (d, $^2J_{C\text{-}P}$ = 6.3 Hz) ppm; **^{31}P{^{1}H} NMR** (121.4 MHz, 20 °C, CD_2Cl_2) δ_P 75.8 (br), –453.6 (br) ppm; **^{31}P{^{1}H} NMR** (121.4 MHz, –90 °C, CD_2Cl_2) δ_P 72.8 (t, *J* = 45.8 Hz), –444.1 (m), –453.0 (m) ppm; **Calc. for $C_{20}H_{27}AuCl_4GaP_5$:** C, 28.91; H, 3.28; Found: C, 31.29; H, 3.69 %. The discrepancy between calculated and observed values for elemental analysis is as a result of placing the sample under vacuum (10^{-2} Torr, 15 mins) as part of the isolation procedure, leading to dissociation and subsequent loss of P_4 and the high values for %C and %H values.

Data for 2: The product crystallises with a single molecule of CH_2Cl_2 in the lattice. This is removed by exposing the sample to vacuum prior to isolation. The following data is for the solvent free material. Crystalline yield 22 mg (46%). **^{1}H NMR** (400 MHz, 20 °C, CD_2Cl_2) δ_H 7.90 (m, Ar*H*, 1H), 7.63 (m, Ar*H*, 2H), 7.25 (m, Ar*H*, 1H), 7.09 (s, Ar*H*, 2H), 3.13 (sep, *J* = 6.9 Hz, C*H*(CH$_3$)$_2$, 1H), 2.35 (sep, *J* = 6.8 Hz, C*H*(CH$_3$)$_2$, 2H), 1.49 (d, *J* = 16.45 Hz, C(CH_3)$_3$, 18H), 1.41 (d, *J* = 6.79 Hz, CH(CH_3)$_2$, 6H), 1.18 (d, *J* = 6.79, CH(CH_3)$_2$, 6H), 0.92 (d, *J* = 6.79 Hz, CH(CH_3)$_2$, 6H) ppm; **^{13}C NMR** (125.7 MHz, 20 °C, CD_2Cl_2) δ_C 135.74 (d, *J* = 8.56 Hz), 132.25 (s), 128.59 (s), 123.56 (s), 39.55 (d, ^1J = 20.10 Hz), 34.55 (s), 31.74 (d, ^2J = 5.59 Hz), 31.48 (s), 26.07 (s), 24.62 (s), 23.92 (s) ppm; **^{31}P{^{1}H} NMR** (121.4 MHz, 20 °C, CD_2Cl_2) δ_P 73.3 (br), –454.8 (br) ppm; **^{31}P{^{1}H} NMR** (121.4 MHz, –90 °C, CD_2Cl_2) δ_P 70.3 (t, *J* = 46.8 Hz), –442.9 (m), –458.4 (m) ppm; **Calc. for $C_{29}H_{45}AuCl_4GaP_5$:** C, 36.40; H, 4.74; Found: C, 36.65; H, 4.87 %.

Reaction Type B: White phosphorus (0.05 mmol, 6 mg) was added to a suspension of 0.05 mmol of LMX (M = Au, X = Cl, L = IPr; M = Cu, X = I, M = Cu, X = I, L = JohnPhos) and $AgSbF_6$ (0.05 mmol, 17 mg) in dichloromethane (3 mL). The suspension was stirred for 1 h in the absence of light then filtered through Celite and washed with dichloromethane (2 × 2 mL). The resulting solutions were concentrated and crystals were grown from CH_2Cl_2/hexane layers. The yields was quantitative by ^{31}P NMR.

Data for 3: Crystalline yield 12 mg (38%). **^{1}H NMR** (400 MHz, 20 °C, CD_2Cl_2) δ_H 7.59 (t, *J* = 7.8 Hz, 2H, Ar*H*), 7.41, (s, 2H, Imid-*H*) 7.37 (d, = 7.8 Hz, 4H, Ar*H*), 2.46 (sep, *J* = 6.9 Hz, 4H, C*H*(CH$_3$)$_2$), 1.26 (d, *J* = 6.9 Hz, CH(CH_3)$_2$), 1.23 (d, *J* = 6.9 Hz, CH(CH_3)$_2$) (overlapped doublet, integral 24H) ppm; **^{31}P{^{1}H} NMR** (121.4 MHz, 20 °C, CD_2Cl_2) δ_P –464.5 (br) ppm; **^{31}P{^{1}H} NMR** (121.4 MHz, –90 °C, CD_2Cl_2) δ_P –450 (br), –460.7 (m) ppm.

Data for 4: Crystalline yield 27 mg (37%).**^{1}H NMR** (500 MHz, 20 °C, CD_2Cl_2) δ_H 7.95-7.91 (1H, m, Ar*H*), 7.71-7.60 (4H, m, Ar*H*), 7.54-7.49 (1H, m, Ar*H*), 7.40-7.36 (2H, m, Ar*H*), 7.35-7.32 (1H, m, Ar*H*), 1.33 (d, $J_{H\text{-}P}$ = 15.5 Hz, 18H, C(CH_3)$_3$) ppm; **^{13}C{^{1}H} NMR** (125.7 MHz, 20 °C, CD_2Cl_2) δ_C 148.62 (d, $J_{C\text{-}P}$ = 19.9 Hz), 143.04 (d, $J_{C\text{-}P}$ = 9.0 Hz), 134.52 (s), 134.09 (s, br), 132.56 (d, $J_{C\text{-}P}$ = 7.26 Hz), 132.29 (d, $J_{C\text{-}P}$ = 2.05 Hz), 129.25(s), 129.21 (s), 127.43 (s), 127.12 (d, $J_{C\text{-}P}$ = 31.89 Hz), 35.86 (d, $^1J_{C\text{-}P}$ = 16.01 Hz), 30.86 (d, $^2J_{C\text{-}P}$ = 7.12 Hz) ppm; **^{31}P{^{1}H} NMR** (202.3 MHz, 20 °C, CD_2Cl_2) δ_P 29.3, –468.9 ppm; **^{31}P{^{1}H} NMR** (121.4 MHz, –90 °C, CD_2Cl_2) δ_P 26.6, –457.8 (br) ppm; **Calc. for $C_{20}H_{27}CuF_6P_5Sb$:** C, 33.29; H, 3.77; Found: C, 33.61; H, 3.54 %

Data for 5: Crystalline yield 25 mg (29%). **^{1}H NMR** (400 MHz, 20 °C, CD_2Cl_2) δ_H 7.93-7.87 (m, Ar*H*, 1H), 7.64-7.59 (m, Ar*H*, 2H), 7.33 (s, Ar*H*, 2H), 7.30-7.26 (m, Ar*H*, 1H), 3.03 (sep, *J* = 6.9 Hz, C*H*(CH$_3$)$_2$, 1H), 2.43 (sep, $J_{H\text{-}P}$ = 6.8 Hz, C*H*(CH$_3$)$_2$, 2H), 1.38 (d, $J_{H\text{-}P}$ = 7.2 Hz, CH(CH_3)$_2$), 1.37 (d, $J_{H\text{-}P}$ = 7.2 Hz, CH(CH_3)$_2$), 1.35 (d, $J_{H\text{-}P}$ = 15.0 Hz,

C(CH_3)$_3$) (overlapping peaks, integral = 30H), 0.96 (d, $J_{H\text{-}P}$ = 6.2 Hz, CH(CH_3)$_2$, 3H); **^{13}C NMR** (125.7 MHz, 20 °C, $CDCl_3$) δ_C 152.38 (s), 147.44 (br), 135.42 (s), 133.72 (d, $J_{C\text{-}P}$ = 7.7 Hz),131.84 (s), 130.18 (s), 129.95 (s), 128.95 (s), 127.03 (br), 36.15 (d, $J_{C\text{-}P}$ = 14.08 Hz), 34.41 (s), 31.85 (s), 31.31 (d, $J_{C\text{-}P}$ = 7.2 Hz), 26.6 (s), 24.20 (s), 23.31 (s) ppm; **^{31}P{^{1}H} NMR** (121.4 MHz, 20 °C, CD_2Cl_2) δ_P 28.6 (br), –492.9 (br) ppm; **^{31}P{^{1}H} NMR** (121.4 MHz, –90 °C, CD_2Cl_2) δ_P 24.4 (br), –452 (br), –466.8 (s) ppm; **Calc. for $C_{29}H_{45}CuF_6P_5Sb$:** C, 41.08; H, 5.35; Found: C, 43.13; H, 5.80 %. The discrepancy between calculated and observed values for elemental analysis is as a result of placing the sample under vacuum (10^{-2} Torr, 15 mins) as part of the isolation procedure, leading to dissociation and subsequent loss of P_4 and the high values for %C and %H values.

Single Crystal X-ray Crystallography

Experiments were performed on **1**-**5** using either a Bruker-AXS SMART APEX three circle diffractometer employing Mo-K$_\alpha$ radiation (λ = 0.71073 Å) or a Microstar diffractometer employing Cu-K$_\alpha$ radiation (λ = 1.5418 Å). Intensities were integrated from several series of exposures, each exposure covering 0.3° in *ω*. Absorption corrections were applied based on multiple and symmetry-equivalent measurements. Hydrogen atoms were constrained to ideal geometries and refined with fixed isotropic displacement parameters. Selected Crystallographic and Data Collection Parameters for Compounds **1**-**5** are shown in Table 2. CCDC 1439692-1439696 contains the supplementary crystallographic data for this paper. These data can be obtained free of charge from The Cambridge Crystallographic Data Centre via www.ccdc.cam.ac.uk/data%5Frequest/cif

Table 2. Selected Crystallographic and Data Collection Parameters for Compounds **1**-**5**.

	1	**2·CH_2Cl_2**	**3**	**4**	**5**
CCDC deposition number	1439692	1439693	1439694	1439695	1439696
Radiation	Cu-K$_\alpha$	Mo-K$_\alpha$	Mo-K$_\alpha$	Mo-K$_\alpha$	Mo-K$_\alpha$
Wavelength (Å)	1.5418	0.71073	0.71073	0.71073	0.71073
Size/mm	0.54×0.11×0.10	0.42×0.28×0.26	0.77×0.11×0.04	0.18×0.17×0.17	0.13×0.11×0.11
Empirical Formula	$C_{20}H_{27}AuCl_4GaP_5$	$C_{30}H_{47}AuCl_6GaP_5$	$C_{27}H_{36}AuF_6N_2P_4Sb$	$C_{20}H_{14}CuF_6P_5Sb$	$C_{29}H_{45}CuF_6P_5Sb$
M	830.75	1041.96	945.17	721.56	847.79
Crystal System	Monoclinic	Triclinic	Monoclinic	Triclinic	Triclinic
Space Group	*P*2(1)/*c*	$P\bar{1}$	*P*2(1)/*n*	$P\bar{1}$	$P\bar{1}$
a/Å	12.2858(19)	8.8067(2)	9.2810(3)	13.3910(6)	8.8000(18)
b/Å	8.8186(14)	12.6087(4)	17.5603(5)	14.2523(6)	14.010(3)
c/Å	26.275(4)	18.7608(5)	20.6174(7)	16.2037(8)	14.490(3)
α/°	90	89.8020(10)	90	91.172(3)	79.77(3)
β/°	96.759(6)	82.2230(10)	95.478(2)	118.927(3)	85.87(3)
γ/°	90	77.8600(10)	90	90.200(3)	83.05(3)
V/Å^3	2826.9(8)	2017.23(10)	3344.82(18)	2705.8(2)	1742.8(6)
Z	4	2	4	4	2
ρ_{calc}/g cm^{-3}	1.952	1.712	1.877	1.771	1.616
μ/mm^{-1}	17.017	4.916	5.434	2.130	1.666
T/K	100(2)	100(2)	100(2)	100(2)	100(2)
$2\theta_{max}$	133.46	55.28	67.34	55.36	67.82
Reflections: total/independent	14937/4855	52426/9381	74936 /12329	13098/13098	11548/11548
R_{int}	0.0441	0.0240	0.0431	-	-
Final *R*1 (I>2σ), *wR*2 (all data)	0.0568, 0.1573	0.0168, 0.0428	0.0249, 0.0424	0.0620, 0.1489	0.0333, 0.0609
Largest peak, hole/eÅ^{-3}	3.477, -1.754	0.764, -0.505	0.974, -1.386	3.718, -1.398	0.599, -0.599

Computational details

All gas-phase calculations on [{P^{t}Bu$_2$(*o*-biphenyl)}Au(η^2-P$_4$)]$^+$, the related intermediates and transition states were performed using the Gaussian 09 software package,[16] with the density functional method BP86.[17] The SDD[18] basis set was used for Au while TZP[19] was used for P, and polarization functions were added (Au: ζ_f = 1.05, P: ζ_d = 0.387).[20] For the six C atoms of the arene ring, the TZP basis set was used while for all the other C and H atoms, SVP[21] was used. The atoms in molecules (AIM) analysis was performed with the AIM2000 software package[22] using an all-electron basis set of double zeta quality (ADZP)[23] for Au, instead of the SDD pseudopotential and associated basis set. Frequency calculations were carried out to verify all of the stationary points as energy minima (zero imaginary frequency) and transition states (one imaginary frequency), and to provide free energies at 298.15 K including entropic contributions. Single point calculations for all the structures were performed with the BP86+D3[24] method with the same basis sets, in order to obtain dispersion-corrected relative free energies. The energies quoted in this paper are all dispersion-corrected unless specifically mentioned.

Acknowledgements

We thank the University of Bristol for funding (L.C.F.), the European Union for funding PhoSciNet through COST Action CM0802, and Rhodia plc for their generous gift of white phosphorus. We thank Dr Martin Murray (Bristol) for his help in modelling nmr spectra.

Keywords: Coinage metals • White phosphorus • Cations • P_4 activation • Density functional theory

[1] a) B. M. Cossairt, N. A. Piro, C. C. Cummins, *Chem. Rev.* **2010**, *110*, 4164-4177; b) M. Caporali, L. Gonsalvi, A. Rossin, M. Peruzzini, *Chem. Rev.* **2010**, *110*, 4178-4235; c) M. Scheer, G. Balazs, A. Seitz, *Chem. Rev.* **2010**, *110*, 4236-4256.

[2] a) I. Krossing, L. van Wüllen, *Chem. Eur. J.* **2002**, *8*, 700-711; b) H. C. Tai, I. Krossing, M. Seth, D. V. Deubel, *Organometallics* **2004**, *23*, 2343-2349; c) P. Dapporto, S. Midollini, L. Sacconi, *Angew. Chem. Int. Ed.* **1979**, *18*, 469-469; d) I. de los Rios, J. R. Hamon, P. Hamon, C. Lapinte, L. Toupet, A. Romerosa, M. Peruzzini, *Angew. Chem. Int. Ed.* **2001**, *40*, 3910-+; e) M. Peruzzini, L. Marvelli, A. Romerosa, R. Rossi, F. Vizza, F. Zanobini, *Eur. J. Inorg. Chem.* **1999**, 931-933.

[3] A. P. Ginsberg, W. E. Lindsell, *J. Am. Chem. Soc.* **1971**, *93*, 2082-2084.

[4] L. C. Forfar, T. J. Clark, M. Green, S. M. Mansell, C. A. Russell, R. A. Sanguramath, J. M. Slattery, *Chem. Commun.* **2012**, *48*, 1970-1972.

[5] a) W. E. Lindsell, K. J. McCullough, A. J. Welch, *J. Am. Chem. Soc.* **1983**, *105*, 4487-4489; b) A. P. Ginsberg, W. E. Lindsell, K. J. McCullough, C. R. Sprinkle, A. J. Welch, *J. Am. Chem. Soc.* **1986**, *108*, 403-416.

[6] B. M. Cossairt, C. C. Cummins, A. R. Head, D. L. Lichtenberger, R. J. F. Berger, S. A. Hayes, N. W. Mitzel, G. Wu, *J. Am. Chem. Soc.* **2010**, *132*, 8459-8465.

[7] a) J. S. Dewar, *Bull. Soc. Chim. Fr.* **1951**, *18*, C71-C79; b) J. Chatt, L. A. Duncanson, *J. Chem. Soc.* **1953**, 2939-2947.

[8] D. V. Deubel, *J. Am. Chem. Soc.* **2002**, *124*, 12312-12318.

[9] L. C. Forfar, T. J. Clark, M. Green, S. M. Mansell, C. A. Russell, R. A. Sanguramath, J. M. Slattery, *Chem. Commun.* **2012**, *48*, 1970-1972.

[10] P. Perez-Galan, N. Delpont, E. Herrero-Gomez, F. Maseras, A. M. Echavarren, *Chem. Eur. J.* **2010**, *16*, 5324-5332.

[11] M. Di Vaira, M. P. Ehses, M. Peruzzini, P. Stoppioni, *Eur. J. Inorg. Chem.* **2000**, 2193-2198.

[12] V. Mirabello, M. Caporali, V. Gallo, L. Gonsalvi, D. Gudat, W. Frey, A. Ienco, M. Latronico, P. Mastrorilli, M. Peruzzini, *Chem. Eur. J.* **2012**, *18*, 11238-11250.

[13] G. Santiso-Quiñones, A. Reisinger, J. Slattery, I. Krossing, *Chem. Commun.* **2007**, 5046-5048.

[14] I. Krossing, *J. Am. Chem. Soc.* **2001**, *123*, 4603-4604.

[15] A. K. Al-Sa'Ady, C. A. McAuliffe, R. V. Parish, J. A. Sandbank, R. A. Potts, W. F. Schneider, in *Inorg. Synth.*, John Wiley & Sons, Inc., **2007**, pp. 191-194.

[16] Gaussian 09, Revision D.01, M. J. Frisch, G. W. Trucks, H. B. Schlegel, G. E. Scuseria, M. A. Robb, J. R. Cheeseman, G. Scalmani, V. Barone, B. Mennucci, G. A. Petersson, H. Nakatsuji, M. Caricato, X. Li, H. P. Hratchian, A. F. Izmaylov, J. Bloino, G. Zheng, J. L. Sonnenberg, M. Hada, M. Ehara, K. Toyota, R. Fukuda, J. Hasegawa, M. Ishida, T. Nakajima, Y. Honda, O. Kitao, H. Nakai, T. Vreven, J. A. Montgomery, Jr., J. E. Peralta, F. Ogliaro, M. Bearpark, J. J. Heyd, E. Brothers, K. N. Kudin, V. N. Staroverov, T. Keith, R. Kobayashi, J. Normand, K. Raghavachari, A. Rendell, J. C. Burant, S. S. Iyengar, J. Tomasi, M. Cossi, N. Rega, J. M. Millam, M. Klene, J. E. Knox, J. B. Cross, V. Bakken, C. Adamo, J. Jaramillo, R. Gomperts, R. E. Stratmann, O. Yazyev, A. J. Austin, R. Cammi, C. Pomelli, J. W. Ochterski, R. L. Martin, K. Morokuma, V. G. Zakrzewski, G. A. Voth, P. Salvador, J. J. Dannenberg, S. Dapprich, A. D. Daniels, O. Farkas, J. B. Foresman, J. V. Ortiz, J. Cioslowski, and D. J. Fox, Gaussian, Inc., Wallingford CT, 2013.

[17] a) A. D. Becke, *Phys. Rev. A* **1988**, *38*, 3098-3100; b) J. P. Perdew, *Phys. Rev. B* **1986**, *33*, 8822-8824.

[18] D. Andrae, U. Haussermann, M. Dolg, H. Stoll, H. Preuss, *Theor. Chim. Acta.* **1990**, *77*, 123-141.

[19] P. L. Barbieri, P. A. Fantin, F. E. Jorge, *Mol. Phys.* **2006**, *104*, 2945-2954.

[20] a) A. W. Ehlers, M. Böhme, S. Dapprich, A. Gobbi, A. Hollwarth, V. Jonas, K. F. Köhler, R. Stegmann, A. Veldkamp, G. Frenking, *Chem. Phys. Lett.* **1993**, *208*, 111-114; b) A. Höllwarth, M. Böhme, S. Dapprich, A. W. Ehlers, A. Gobbi, V. Jonas, K. F. Köhler, R. Stegmann, A. Veldkamp, G. Frenking, *Chem. Phys. Lett.* **1993**, *208*, 237-240.

[21] A. Schafer, H. Horn, R. Ahlrichs, *J. Chem. Phys.* **1992**, *97*, 2571-2577.

[22] F. Biegler-Konig, J. Schonbohm, D. Bayles, *J Comput Chem* **2001**, *22*, 545-559.

[23] A. C. Neto, F. E. Jorge, *Chem. Phys. Lett.* **2013**, *582*, 158-162.

[24] S. Grimme, J. Antony, S. Ehrlich, H. Krieg, *J. Chem. Phys.* **2010**, *132*.

Entry for the Table of Contents (Please choose one layout)

FULL PAPER

A series of cationic white phosphorus complexes of the coinage metals Au and Cu have been synthesised and investigated both in the solid state and in solution. Electronic structure calculations have been used to probe both static and dynamic features of the complexes.

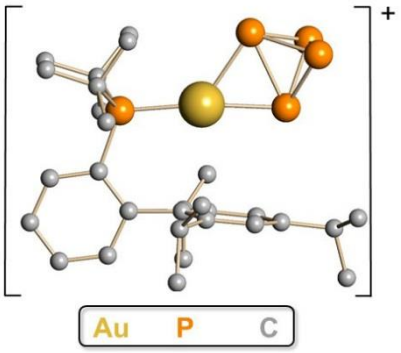

Laura C. Forfar, Dihao Zeng, Michael Green, John E. McGrady and Christopher A. Russell**

Page No. – Page No.

Probing the Structure, Dynamics and Bonding of Coinage Metal Complexes of White Phosphorus